Received: 17 August 2017 | Revised: 13 November 2017 | Accepted: 17 November 2017
DOI: 10.1111/ter.12317

PAPER

WILEY Terra Nova

Non-uniform splitting of a single mantle plume by double cratonic roots: Insight into the origin of the central and southern East African Rift System

Alexander Koptev[1,2] | Sierd Cloetingh[3] | Taras Gerya[4] | Eric Calais[5] | Sylvie Leroy[1]

[1]Sorbonne Universités, UPMC Univ Paris 06, CNRS, Institut des Sciences de la Terre de Paris (iSTeP), Paris, France

[2]Department of Geosciences, University of Tübingen, Tübingen, Germany

[3]Department of Earth Sciences, Utrecht University, Utrecht, The Netherlands

[4]ETH-Zurich, Institute of Geophysics, Zurich, Switzerland

[5]Ecole Normale Supérieure, Department of Geosciences, PSL Research University, CNRS, UMR 8538, Paris, France

Correspondence
Alexander Koptev, Department of Geosciences, University of Tübingen, Tübingen, Germany.
Email: alexander.koptev@ifg.uni-tuebingen.de

Funding information
Advanced ERC Grant RHEOLITH, Grant/Award Number: 290864; ERC Consolidator Grant EXTREME, Grant/Award Number: 615703; U.S. National Science Foundation, Grant/Award Number: EAR-0538119; French INSU197 CNRS

Abstract

Using numerical thermo-mechanical experiments we analyse the role of an active mantle plume and pre-existing lithospheric thickness differences in the structural development of the central and southern East African Rift system. The plume-lithosphere interaction model setup captures the essential features of the studied area: two cratonic bodies embedded into surrounding lithosphere of normal thickness. The results of the numerical experiments suggest that localization of rift branches in the crust is mainly defined by the initial position of the mantle plume relative to the cratons. We demonstrate that development of the Eastern branch, the Western branch and the Malawi rift can be the result of non-uniform splitting of the Kenyan plume, which has been rising underneath the southern part of the Tanzanian craton. Major features associated with Cenozoic rifting can thus be reproduced in a relatively simple model of the interaction between a single mantle plume and pre-stressed continental lithosphere with double cratonic roots.

1 | INTRODUCTION

The East African Rift system (EARS; Braile, Keller, Wendlandt, Morgan, & Khan, 2006; Chorowicz, 2005; McConnell, 1972; Ring, 2014) has two branches, the Eastern branch and the Western branch. The N–S-oriented Eastern branch (Baker, 1987; Baker, Mohr, & Williams, 1972; Ebinger, 2005; Keller et al., 1991; Mechie, Keller, Prodehl, Khan, & Gaciri, 1997; Smith, 1994; Williams, 1982) extends over 2,000 km from the Afar Triple Junction (McClusky, Reilinger, Mahmoud, Sari, & Tealeb, 2003; Mohr, 1970) in the north to the North Tanzanian Divergence Zone (Dawson, 1992; Isola, Mazzarini, Bonini, & Corti, 2014; Le Gall et al., 2004, 2008) in the south (Figure 1) and consists of the relatively narrow Main Ethiopian rift (Keranen, Klemperer, Julia, Lawrence, & Nyblade, 2009), the wide rift in the Turkana depression (Morley et al., 1992) and a narrow rift at the Tanzanian craton margin in the Kenya rift (Zeyen et al., 1997). In the present study, however, we consider only the southern part of the Eastern branch from northern Kenya to north-eastern Tanzania. The Western branch (Bauer et al., 2013; Daly, Chorowicz, & Fairhead, 1989; Ebinger, 1989; Morley, Cunningam, Wescott, & Harper, 1999; Pasteels, Villeneuve, De Paepe, & Klerkx, 1989) is composed of the Albert-Edward, Kivu and Tanganyika-Rukwa rifts, oriented in NE–SW, N–S and NW–SE directions, respectively, depicting an arcuate map-trace along the western side of the Tanzanian craton (Figure 1). The southern prolongation of the Western branch is represented by the Malawi rift (Laó-Dávila, Al-Salmi, Abdelsalam, & Atekwana, 2015; Ring, Betzler, & Delvaux, 1992), which is aligned on a N–S trend extending from the Rungwe volcanic province (southern Tanzania) to the Urema graben (Mozambique). Geological estimates indicate a higher degree of total lithospheric extension in the Kenya rift than in

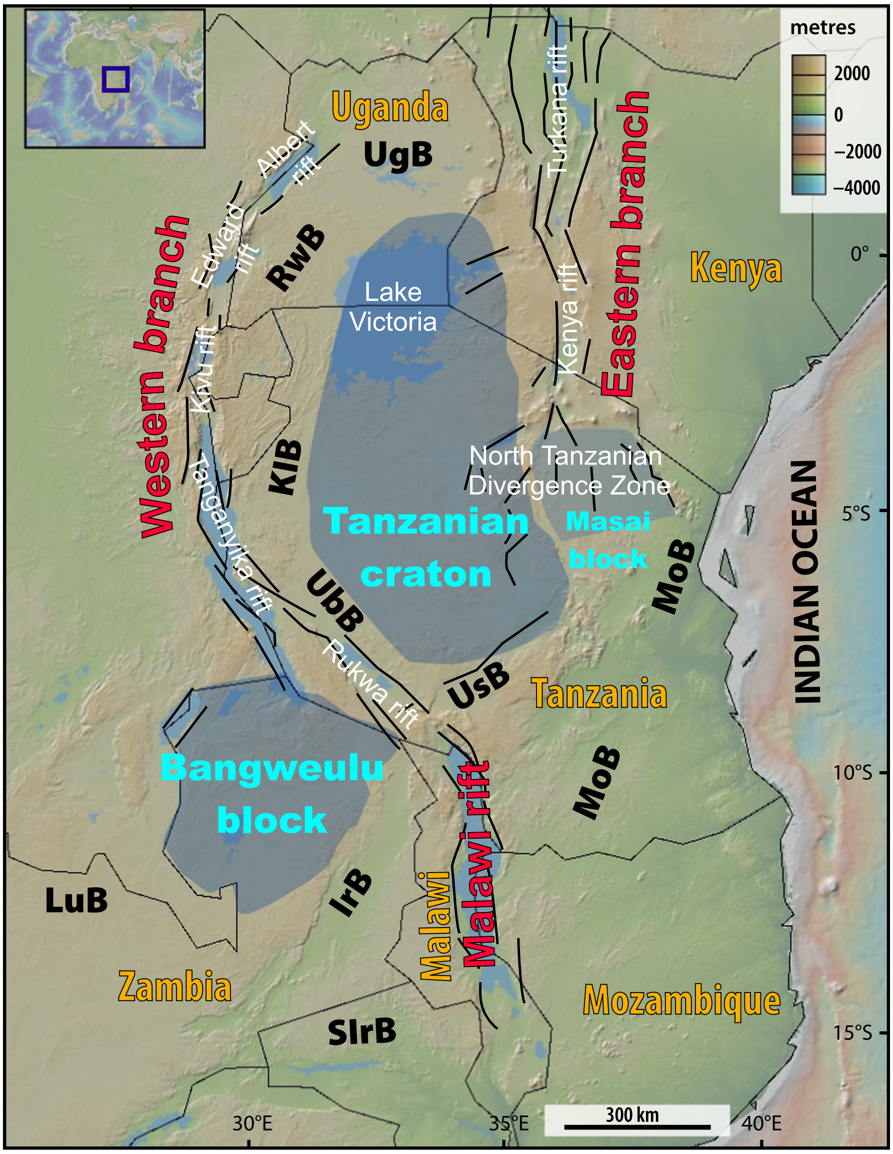

FIGURE 1 Topographic map showing the tectonic setting of the central and southern EARS (after Mulibo & Nyblade, 2013b and Corti et al., 2013), which comprises the Tanzanian craton (likely including the Uganda Basement Complex [UgB]), the Bangweulu block, the Masai block and several Proterozoic orogenic belts: Rwenzori (RwB), Kibaran (KiB), Ubendian (UbB), Usagaran (UsB), Mozambique (MoB), Iruminde (IrB), Southern Iruminde (SIrB), Lufilian (LuB). Black lines show major faults (Corti et al., 2013). The inset indicates the location of the studied area [Colour figure can be viewed at wileyonlinelibrary.com]

the Western branch and the North Tanzanian Divergence Zone (Ring, 2014 and references therein).

The Western and Eastern branches are separated by the Archaean (2,500–3,000 Ma) Tanzanian craton (Bell & Dodson, 1981; Chesley, Rudnick, & Lee, 1999; Manya, 2011), characterized by a strong and cold lithosphere with a 150–300-km-thick keel (Adams, Nyblade, & Weeraratne, 2012; Artemieva, 2006; Mulibo & Nyblade, 2013a, 2013b). The 175-km-thick (Artemieva, 2006) Archaean–Palaeoproterozoic Bangweulu block (Andersen & Unrug, 1984; De Waele, Liégeois, Nemchin, & Tembo, 2006), which has been stable since 1,750 Ma (Lenoir, Liégeois, Theunissen, & Klerkx, 1994), lies to the south-west of the Tanzanian craton. The Tanzanian and Bangweulu cratons are both surrounded by Proterozoic orogenic belts (Begg et al., 2009; Cahen, Snelling, Delhal, & Vail, 1984) with a relatively thin (≤150 km) thermal lithosphere (Artemieva, 2006; Koptev & Ershov, 2011).

Geophysical (e.g., Nolet, Karato, & Montelli, 2006; Nyblade, Owens, Gurrola, Ritsema, & Langston, 2000; Ritsema, Nyblade, Owens, & Langston, 1998) and geochemical (e.g., Armitage et al., 2015; Rooney, Herzberg, & Bastow, 2012) observations indicate the presence of mantle plumes under the EARS, possibly rooted into a common deep-mantle anomaly (Ritsema, van Heijst, & Woodhouse, 1999) corresponding to the African superplume. However, the actual number of plumes and their relative positions within this broad upwelling region remain contentious (e.g., Chang, Ferreira, Ritsema, van Heijst, & Woodhouse, 2015; Chang & Van der Lee, 2011; Civiero et al., 2016; Weeraratne, Forsyth, Fischer, & Nyblade, 2003).

It is commonly assumed that the Cenozoic rifts have avoided the cratons and follow the mobile belts (McConnell, 1972; Mohr, 1982), which serve as the weakest pathways for rift propagation. Structural control exerted by the pre-existing heterogeneities within the Proterozoic belts at the scale of individual faults or rifts has also been demonstrated (Corti, van Wijk, Cloetingh, & Morley, 2007; Katumwehe, Abdelsalam, & Atekwana, 2015; Morley, 2010; Ring, 1994; Smets et al., 2016; Theunissen, Klerkx, Melnikov, & Mruma, 1996; Versfelt & Rosendahl, 1989).

However, as shown by Koptev, Calais, Burov, Leroy, and Gerya (2015), Koptev et al. (2016), the formation of two rift zones on opposite sides of a thick lithosphere segment can be explained without appealing to pre-imposed heterogeneities at the crustal level.

TABLE 1 Controlling parameters of the models

			Controlling parameters				
Model number	Model series	Model title	Tanzanian craton shape	Plume position (az/shift, km)	Presence of the Masai block	Stronger lower crust for cratons	Figure
1	General	*Sym.No plume*	Symmetrical	—	No	No	3
2	General	*Sym.W/10,S/230*	Symmetrical	W/10, S/230	No	No	4a
3	General	*Sym.S/230*	Symmetrical	E/0, S/230	No	No	4b
4	General	*Sym.E/10,S/230*	Symmetrical	E/10, S/230	No	No	4c
5	General	*Asym.W/10,S/230*	Asymmetrical	W/10, S/230	No	No	4d
6	General	*Asym.S/230*	Asymmetrical	E/0, S/230	No	No	4e
7	General	*Asym.E/10,S/230*	Asymmetrical	E/10, S/230	No	No	4f
8	General	*Asym.E/20,S/230*	Asymmetrical	E/20, S/230	No	No	4g
9	General	*Asym.E/20,S/220*	Asymmetrical	E/20, S/220	No	No	4h and 5
10	General	*Asym.E/20,S/210*	Asymmetrical	E/20, S/210	No	No	4i
11	General	*Asym.E/30,S/230*	Asymmetrical	E/30, S/230	No	No	4j
12	General	*Asym.E/30,S/220*	Asymmetrical	E/30, S/220	No	No	4k
13	General	*Asym.E/30,S/210*	Asymmetrical	E/30, S/210	No	No	4l
14	Complementary	*Asym.E/20,S/220; with Masai*	Asymmetrical	E/20, S/220	Yes	No	6a
15	Complementary	*Asym.E/30,S/210; with Masai*	Asymmetrical	E/30, S/210	Yes	No	6b
16	Complementary	*Asym.E/20,S/220; with diff. crust*	Asymmetrical	E/20, S/220	No	Yes	6c
17	Complementary	*Asym.E/30,S/210; with Masai+diff. crust*	Asymmetrical	E/30, S/210	Yes	Yes	6d

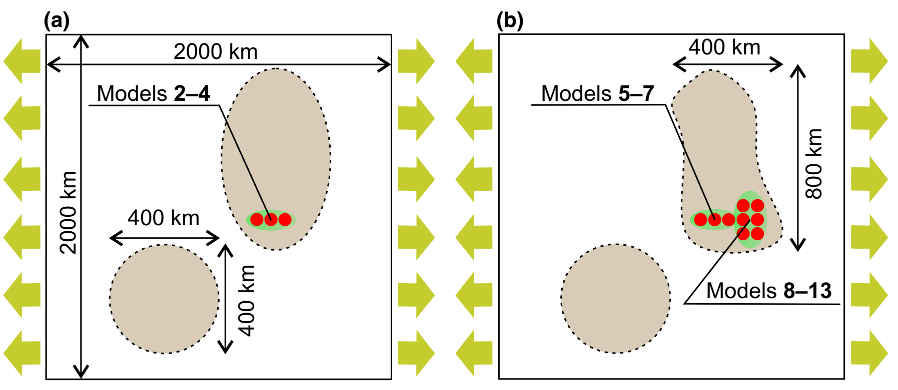

FIGURE 2 Model setups for the general model series shown in Figure 4. (a) Models **2**–**4**, characterized by a simple quasi-rectangular shape of the Tanzanian craton as in previously published experiments (Koptev et al., 2015, 2016). (b) Models **5**–**13**, with a more complex asymmetrical configuration of the Tanzanian block (based on its present-day surface outline). Initial plume positions are shown by red circles within tested areas (shaded green) with respect to cratonic blocks (grey ellipses). "No-plume" model **1** (see Figure 3) is characterized by a simple symmetrical configuration of the Tanzanian craton and by the absence of a pre-imposed mantle plume anomaly. The initial model setup and geotherm were adopted with respect to observation-based models of regional thermal and rheological structure of the continental lithosphere in East Africa (Albaric, Déverchère, Petit, Perrot, & Le Gall, 2009; Artemieva, 2006; Fishwick & Bastow, 2011; Pérez-Gussinyé et al., 2009). Rheological parameters were chosen in consideration of extensive and successful experience obtained from heterogeneous continental rifting (e.g., Huismans & Beaumont, 2007; Wenker & Beaumont, 2016 and references therein) and plume–lithosphere interaction modelling (e.g., Beniest, Koptev, & Burov, 2017; Beniest, Koptev, Leroy, Sassi, & Guichet, 2017; Burov, 2011; Burov & Cloetingh, 2010; Burov & Gerya, 2014; Burov & Guillou-Frottier, 2005; Burov, Guillou-Frottier, d'Acremont, Le Pourhiet, & Cloetingh, 2007; Koptev, Burov, et al., 2017; Koptev, Cloetingh, Burov, François, & Gerya, 2017) including our previous Africa-oriented experiments (Koptev et al., 2015, 2016), which have been able to reproduce a number of key features of the central EARS such as timing, surface velocity distribution and large-scale topography [Colour figure can be viewed at wileyonlinelibrary.com]

Their models have provided a unified physical framework to understand the simultaneous development of the Western and Eastern branches around a thicker Tanzanian craton (Roberts et al., 2012) as a result of the interaction between pre-stressed continental lithosphere and a single mantle plume anomaly corresponding to the Kenyan plume (Chang & Van der Lee, 2011; George, Rogers, &

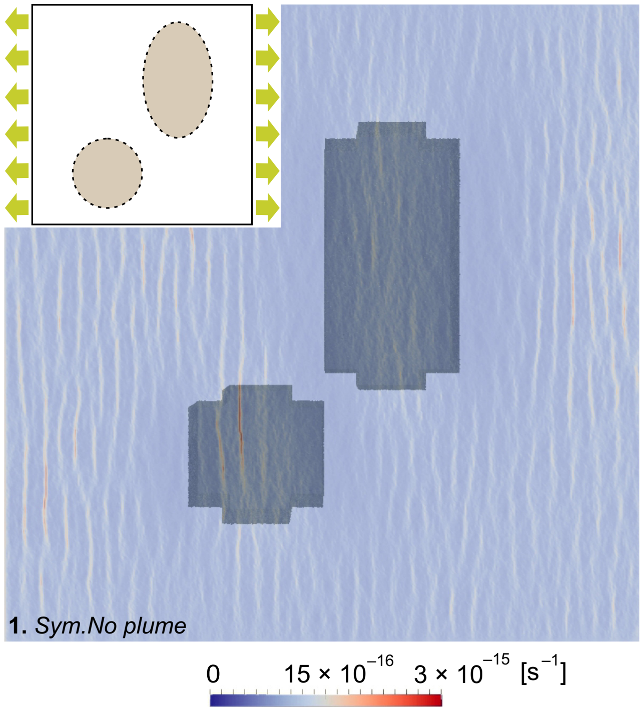

FIGURE 3 "No-plume" model **1** at 5 Ma. Blue to red colours indicate crustal strain rate. The cratons are the dark grey volumes. Unidirectional tectonic stretching of the continental lithosphere in the absence of active mantle upwelling results in distributed closely spaced small-offset parallel faults, which are not localized within any particular zone. Upper crustal distributed deformation covers all model domains uniformly (including the cratonic areas) because of the lateral homogeneity of the crustal composition adopted in the general model series. Note that progressive focusing and amplification of localized non-axisymmetric deformation is generated only by the simultaneous presence of hot plume material underneath the lithosphere basement and passive horizontal extension, while mantle plume impingement on non-pre-stressed lithosphere can only result in axisymmetric domal-shaped features with multiple radiating rifts (see Burov & Gerya, 2014 for more detail) [Colour figure can be viewed at wileyonlinelibrary.com]

Kelley, 1998; Pik, Marty, & Hilton, 2006). Yet, the southern prolongation of the Western rift by the Malawi rift has not been reproduced in any of these "one-craton" experiments (Koptev et al., 2015, 2016). In order to overcome this discrepancy, we follow-up on our previous studies with a series of laterally widened thermo-mechanical models characterized by the presence of a second zone of lithospheric thickening that roughly mimics the isometric (i.e. having equal horizontal dimensions) Bangweulu block situated south-west of the Tanzanian craton and by a single mantle plume seeded underneath the southern part of the Tanzanian craton (e.g., Bagley & Nyblade, 2013; Hansen, Nyblade, & Benoit, 2012).

2 | MODEL AND EXPERIMENTS

Our modelling is based on the thermo-mechanical viscous–plastic 3DELVIS code (Gerya & Yuen, 2007), which combines the finite difference method with a marker-in-cell technique (see Gerya, 2010 for more details).

The 3D model box encompasses the entire 650-km-deep upper mantle, with large horizontal scales (2,000 × 2,000 km), and offers "lithospheric-scale" resolution (~5 km × 5 km × 5 km per grid cell). The initial model setup corresponds to the onset of a stratified three-layer (upper/lower crust and lithospheric mantle) continental lithosphere, which is underlain by asthenospheric upper mantle. The initial geotherm is piece-wise linear, with 0°C at the surface, 700°C at the Moho, 1,300°C at the lithosphere–asthenosphere boundary and 1,630°C at the bottom of the model box. The mantle plume is initiated by a temperature anomaly of +370°C at the base of the upper mantle. In all presented experiments, we applied a constant E–W extension with a half rate of 3 mm/yr, a typical value for pre-break-up continental rifts, including the Nubia-Somalia plate system (Saria, Calais, Stamps, Delvaux, & Hartnady, 2014; Stamps et al., 2008).

The general model series (Table 1; models **1**–**13**) is characterized by lateral homogeneity of the crustal composition and by the presence of two 250-km-thick cratons embedded into surrounding "normal" (150 km thick) lithosphere. The first cratonic block is elongated in a N–S direction (horizontal dimensions are 400 × 800 km) roughly mimicking the configuration of the Tanzanian craton, whereas the second one is small and isometric (horizontal dimensions are 400 × 400 km) corresponding to the Bangweulu block. The initial plume location represents a key controlling parameter of our study (Figure 2). In all performed experiments (except for "no-plume" model **1**; Figure 3) the mantle plume was shifted to the south up to 230 km with respect to the centre of the Tanzanian craton. We have studied the impact of small lateral variations in its initial position: the southward shift varies from 210 to 230 km whereas the latitudinal displacement is from 10 km to the west to 30 km to the east; different configurations of the Tanzanian craton have been tested as well (Table 1; Figures 4 and 5). In order to investigate the potential role of second-order structural heterogeneities we performed several complementary experiments (models **14**–**17**, Figure 6) including stronger (plagioclase flow law instead of wet quartzite flow law) lower crust within the cratonic blocks (models **16, 17**) and/or a third zone of lithospheric thickening situated to the west of the Tanzanian craton and roughly mimicking the size and configuration of the Masai block (models **14, 15**, **17**).

3 | RESULTS AND DISCUSSION

As in previous 3D experiments (Burov & Gerya, 2014; Koptev et al., 2015, 2016), the models presented here predict a rapid mantle ascent as the mantle plume reaches the lithospheric bottom after 0.5 Ma. The common feature of the performed models is a separation of the upwelling plume head into three parts by the lithosphere of the Tanzanian and Bangweulu blocks. After being divided, the buoyant plume material ponds at the base of "normal" lithosphere adjacent to the western, eastern and southern sides of the Tanzanian craton (Figure 4).

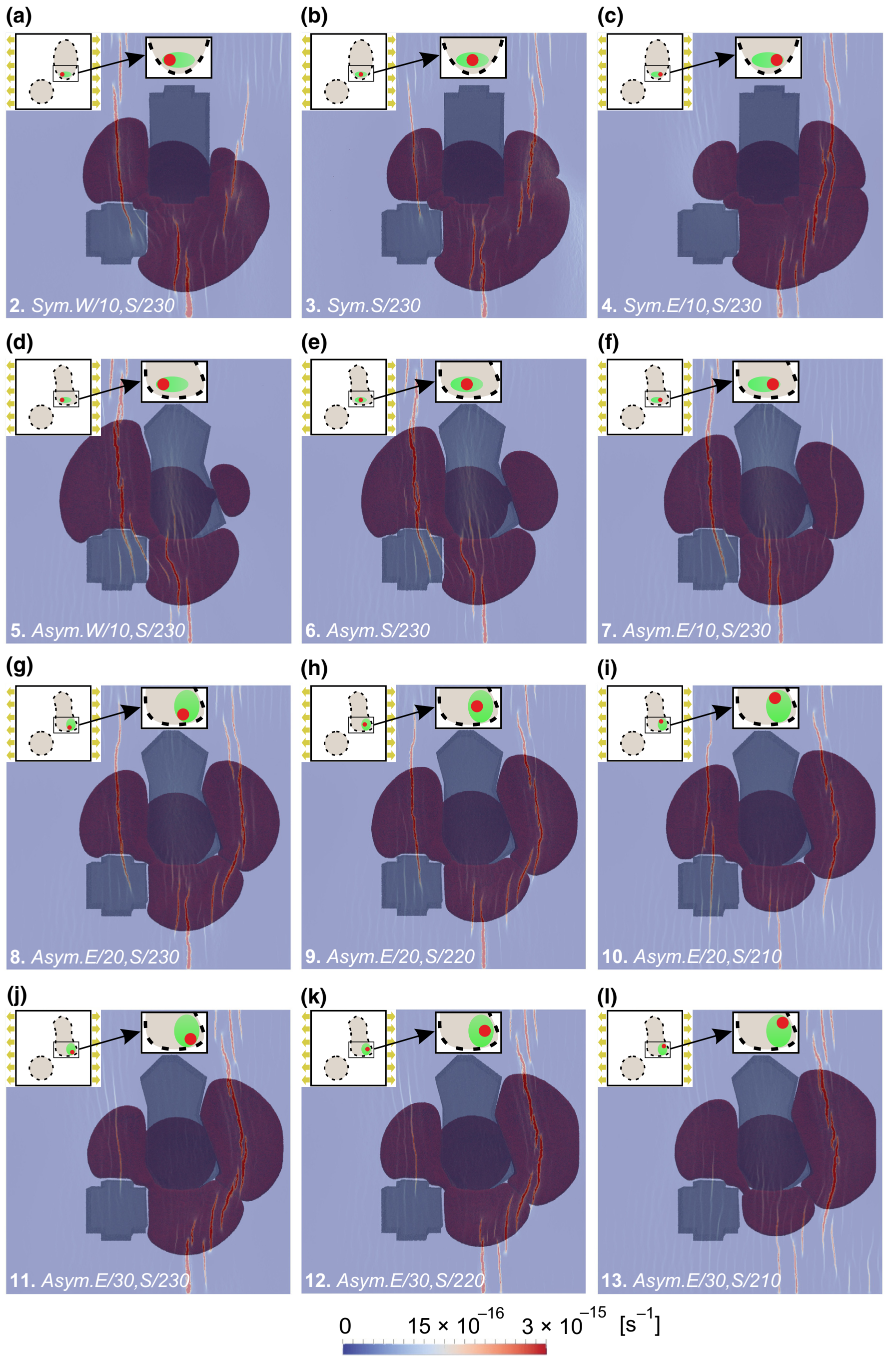

FIGURE 4 Top view of the results of 3D experiments **2**–**13** at 5–10 Ma. The plume material is shown in dark red. Left-top insets schematically illustrate the initial position of the mantle plume. Note that the relative positions of lithospheric heterogeneities and the initial mantle plume anomaly appear to be the crucial factor controlling the resulting rifting pattern [Colour figure can be viewed at wileyonlinelibrary.com]

In the absence of active mantle upwelling ("no-plume" model **1**), ultra-slow tectonic extension can only result in broadly distributed small-offset parallel faults (Figure 3). On the contrary, in most of the other experiments (Figure 4), the continental crust above the hot plume material is subjected to localized brittle deformation forming three linear, 100–500-km-long rifting centres stretched perpendicular to the external E–W extension. As already shown by Burov and Gerya (2014), such large-scale linear normal faults are triggered and maintained by mantle flow that impacts the bottom of the continental lithosphere.

The degree of development (in terms of modelled strain rates) of each of these branches is directly controlled by the relative amount of hot plume material ponding underneath the corresponding lithosphere segment (Figure 4). In certain cases, however, this amount appears to be too small to localize any visible deformation in the crust. For example, the plume's eastward shift of 10 km in combination with the simplified shape of the Tanzanian craton results in the absence of a discernible western rift (model **4**, Figure 4c). Similarly, the eastern branch is not reproduced in the experiments assuming a more realistic Tanzanian craton and the mantle plume with initial latitudinal displacement of 0 or 10 km to the west (models **6** and **5**, respectively; Figure 4e,d). Only the plume's eastward shift up to 20 km (models **8**–**10**; Figure 4g–i) can provide a symmetrical rifting on both (eastern and western) sides of the Tanzanian craton. Further

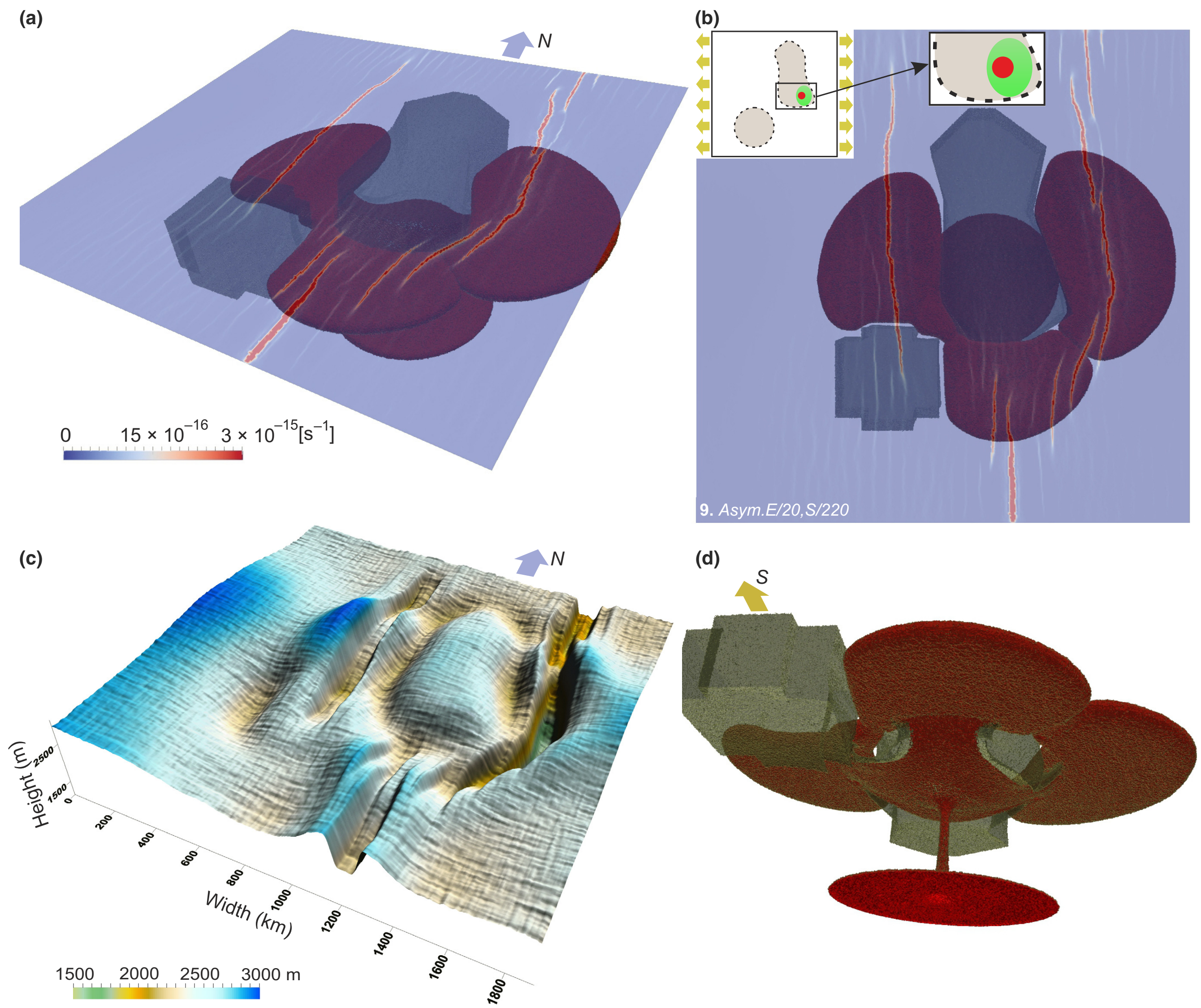

FIGURE 5 The “best-fit” experiment **9** (*Asym.E/20,S/220*) of the general model series: (a) 3D view; (b) top view; (c) corresponding surface topography; (d) bottom view. Note that the strain distribution bears strong similarities to the central and southern EARS, showing the “three-branches” pattern with simultaneous development of the Eastern branch, the Western branch and the Malawi rift [Colour figure can be viewed at wileyonlinelibrary.com]

plume displacement to the east (up to 30 km) leads to a more developed eastern branch compared to the western one (models **11**–**13**; Figure 4j–l). The southern rift zone situated east of the Bangweulu block is expressed clearly in all models. Note, however, that it becomes less pronounced when the plume's southward shift decreases from 230 to 210 km (compare models **8**; Figure 4g) and **10** (Figure 4i) or models **11** (Figure 4j) and **13** (Figure 4l). The asymmetrical distribution of hot mantle material on the opposite sides of the craton (e.g., models **11** and **12**) can provoke contrasted magmatic activity as observed in the central EARS, explaining a magma-rich Eastern branch and a magma-poor Western branch (e.g., Chorowicz, 2005; Ring, 2014).

We have identified model **9** (Figures 4h and 5) as the “best-fit” experiment of the general model series (models **1**–**13**) because it reproduces all three rift zones, which are clearly reflected not only in the strain-rate field but also in the surface topography (Figure 5c). Several other models (such as models **3** or **8**), however, could also be considered as the “best-fit” (Figure 4b,g) because they are also able to reproduce synchronous growth of the Eastern branch, the Western branch and the Malawi rift. Note that modelled accumulated deformation in the localized rift basins amounts to several tens of km of total extension, which is in accord with geological estimates for the central part of the EARS (e.g.. Ring, 2014 and references therein). A striking feature is the consistency between modelled and observed rift distributions in the case where the Kenyan plume is seeded underneath the southern part of the Tanzanian craton.

A principal shortcoming of this “best-fit” experiment (model **9**; Figure 5) is that it does not reproduce the NW–SE-oriented Rukwa

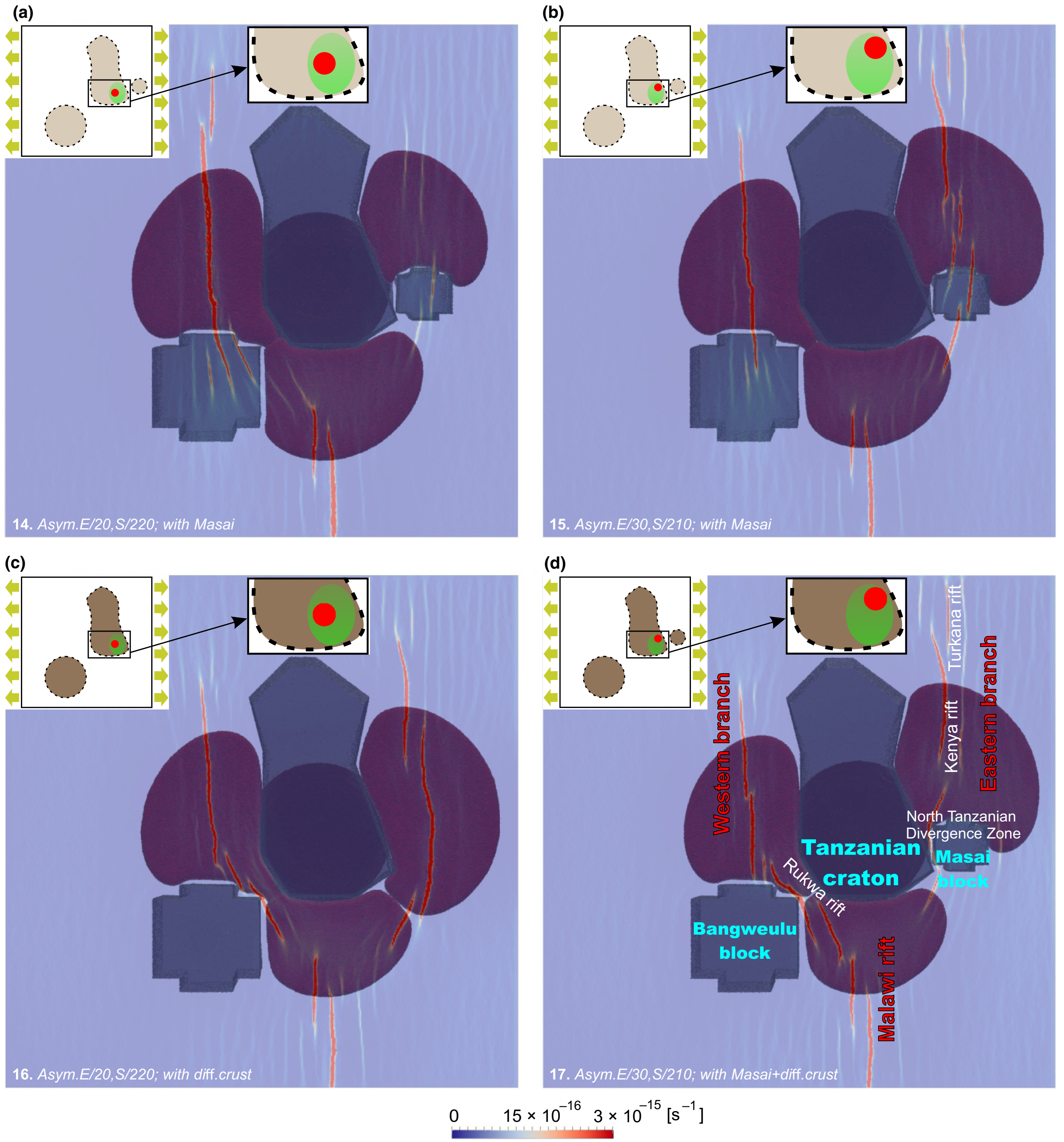

FIGURE 6 Top view of the complementary models **14**–**17** at 5–10 Ma. Complementary models differ from the general model series (models **1**–**13**; Figures 4 and 5) by: (a, b, d) the presence of a third area of lithospheric thickening corresponding to the Masai block (models **14**, **15** and **17**) and/or by (c, d) a stronger rheology for the lower crust within cratonic areas (models **16** and **17**). Note that these experiments containing more predefined complexities provide better fitting with the observed data than do the experiments of the general model series. In particular, model **17** reproduces not only three first-order rift structures corresponding to the Eastern branch, the Western branch and the Malawi rift but also second-order features such as the NW–SE-oriented Rukwa rift and the along-axis transition observed between the narrow Kenya rift and the broader Turkana depression to the north and the multi-basin North Tanzania Divergence Zone to the south (compare Figures 1 and 6d) [Colour figure can be viewed at wileyonlinelibrary.com]

rift segment of the Western branch (Figure 1). Similarly to most of the other models, the southern end of the western branch penetrates into the area underlain by the Bangweulu block. In this case, thick lithosphere appears not to be resistant to lateral propagation of localized deformation given the homogenous crustal composition adopted in the general model series, where the crustal rheology of the cratonic blocks does not differ from that of the surrounding "normal" lithosphere. The situation changes completely when not only thicker lithospheric mantle but also stronger rheology of the lower crust is considered for the cratonic areas (complementary model series: models **16** and **17**, Figure 6c,d): in this case, localized strain tends to avoid the strong cratons, leaving them almost undeformed. In particular, this leads to a change in orientation from N–S to NW–SE for the southernmost segment of the western branch (corresponding to the Rukwa rift) thus providing a framework much more consistent with the observed data. Introduction of the Masai block, for its part, improves the relative location of widening of the rift zone in the southern segment of the eastern branch (models **15** and **17**; Figure 6b,d) corresponding to the observed transition between the narrow Kenya rift and a considerably wider zone (300–400 km) of block faulting in northern Tanzania (Corti, Iandelli, & Cerca, 2013; Dawson, 1992; Ebinger, Poudjom, Mbede, Foster, & Dawson, 1997; Foster, Ebinger, Mbede, & Rex, 1997; Le Gall et al., 2008).

It should be noted that given the better fit with the observed data in complementary models containing more predefined complexities (see Figure 6d), the analysed plume-induced multi-branch continental rifting dynamics need further numerical investigation and quantitative analysis of the controlling factors, including the complex 3D structure of the central EARS in terms of inherited compositional and rheological heterogeneities of the crust and lithospheric mantle (e.g., Sippel et al., 2017).

4 | CONCLUSIONS

The fully coupled thermo-mechanical models presented here start from relatively simple initial conditions: a single mantle plume anomaly seeded underneath the continental lithosphere embedding two cratonic blocks. These experiments evolve over time to create a complex system characterized by asymmetrical splitting of the plume head into three parts. The resulting relative distribution of hot plume material ponding below "normal" lithosphere is a controlling parameter for localizing deformation at the crustal level. Very small variations in initial plume position with respect to the cratonic bodies (up to several tens of km only) appear to be able to change the relation between these three segments of separated plume head, which, in turn, alters the degree of development of the corresponding rift branches. We argue, thus, that the resulting rifting pattern is largely controlled by the relative position of the initial mantle plume anomaly with respect to first-order lithospheric thickness differences rather than by second-order crustal and/or lithospheric compositional heterogeneities as commonly assumed (Corti et al., 2007; Katumwehe et al., 2015; Smets et al., 2016; Theunissen et al., 1996).

The performed analysis permits us to identify an initial model configuration that results in a strain distribution that bears strong similarities to the central and southern EARS, showing simultaneous development of the Eastern branch, the Western branch and its southern prolongation by the Malawi rift. The number and relative positions of rift branches with respect to the cratons within the studied area can be explained by the impact of a single mantle anomaly on pre-stressed continental lithosphere that does not contain any pre-defined heterogeneities other than the well-known cratonic blocks.

ACKNOWLEDGEMENTS

We thank Judith Sippel and two anonymous reviewers for their helpful comments during the preparation of this paper. A. Koptev acknowledges support from the ERC Advanced Grant 290864 RHEOLITH and ERC Consolidator Grant 615703 EXTREME. S. Cloetingh was supported through a UPMC visiting professor grant. E. Calais acknowledges support from U.S. National Science Foundation grant EAR-0538119 and the French INSU197 CNRS program Tellus-Rift. The numerical simulations were performed on the ERC-funded SGI Ulysse cluster of ISTEP.

ORCID

Alexander Koptev http://orcid.org/0000-0002-3246-5764
Sierd Cloetingh http://orcid.org/0000-0001-9472-7881
Taras Gerya http://orcid.org/0000-0002-1062-2722
Eric Calais http://orcid.org/0000-0002-5935-8117
Sylvie Leroy http://orcid.org/0000-0002-3188-8802

REFERENCES

Adams, A., Nyblade, A., & Weeraratne, D. (2012). Upper mantle shear wave velocity structure beneath the East African plateau: Evidence for a deep, plateauwide low velocity anomaly. *Geophysical Journal International*, *189*, 123–142.

Albaric, J., Déverchère, J., Petit, C., Perrot, J., & Le Gall, B. (2009). Crustal rheology and depth distribution of earthquakes: Insights from the central and southern East African Rift System. *Tectonophysics*, *468*, 28–41.

Andersen, L. S., & Unrug, R. (1984). Geodynamic evolution of the Bangweulu Block, northern Zambia. *Precambrian Research*, *25*, 187–212.

Armitage, J. J., Ferguson, D. J., Goes, S., Hammond, J. O. S., Calais, E., Rychert, C. A., & Harmon, N. (2015). Upper mantle temperature and the onset of extension and break-up in Afar, Africa. *Earth and Planetary Science Letters*, *418*, 78–90.

Artemieva, I. M. (2006). Global 1 × 1 thermal model TC1 for the continental lithosphere: Implications for lithosphere secular evolution. *Tectonophysics*, *416*, 245–277.

Bagley, B., & Nyblade, A. A. (2013). Seismic anisotropy in eastern Africa, mantle flow, and the African superplume. *Geophysical Research Letters*, *40*, 1500–1505.

Baker, B. H. (1987). Outline of the petrology of the Kenya rift alkaline province. *Geological Society, London, Special Publications*, *30*, 293–311.

Baker, B. H., Mohr, P. A., & Williams, L. A. J. (1972). Geology of the eastern rift system of Africa. *Geological Society of America Special Papers*, *136*, 1–68.

Bauer, F. U., Glasmacher, U. A., Ring, U., Karl, M., Schumann, A., & Nagudi, B. (2013). Tracing the exhumation history of the Rwenzori Mountains, Albertine Rift, Uganda, using low temperature thermochronology. *Tectonophysics*, *599*, 8–28.

Begg, G. C., Griffin, W. L., Natapov, L. M., O'Reilly, S. Y., Grand, S. P., O'Neill, C. J. ... Bowden, P. (2009). The lithospheric architecture of

Africa: Seismic tomography, mantle petrology, and tectonic evolution. *Geosphere*, *5*, 23–50.

Bell, K., & Dodson, M. H. (1981). The geochronology of the Tanzanian shield. *The Journal of Geology*, *89*, 109–128.

Beniest, A., Koptev, A., & Burov, E. (2017). Numerical models for continental break-up: Implications for the South Atlantic. *Earth and Planetary Science Letters*, *461*, 176–189.

Beniest, A., Koptev, A., Leroy, S., Sassi, W., & Guichet, X. (2017). Two-branch break-up systems by a single mantle plume: Insights from numerical modeling. *Geophysical Research Letters*, *44*, 9589–9597.

Braile, L. W., Keller, G. R., Wendlandt, R. F., Morgan, P., & Khan, M. A. (2006). The East African rift system. *Developments in Geotectonics*, *25*, 213–III.

Burov, E. (2011). Rheology and strength of the lithosphere. *Marine and Petroleum Geology*, *28*, 1402–1443.

Burov, E., & Cloetingh, S. (2010). Plume-like upper mantle instabilities drive subduction initiation. *Geophysical Research Letters*, *37*, L03309.

Burov, E., & Gerya, T. (2014). Asymmetric three-dimensional topography over mantle plumes. *Nature*, *513*, 85–89.

Burov, E., & Guillou-Frottier, L. (2005). The plume head–continental lithosphere interaction using a tectonically realistic formulation for the lithosphere. *Geophysical Journal International*, *161*, 469–490.

Burov, E., Guillou-Frottier, L., d'Acremont, E., Le Pourhiet, L., & Cloetingh, S. (2007). Plume head-lithosphere interactions near intra-continental plate boundaries. *Tectonophysics*, *434*, 15–38.

Cahen, L., Snelling, N., Delhal, J., & Vail, J. (1984). *The geochronology and evolution of Africa*. New York, NY: Oxford University Press.

Chang, S. J., Ferreira, A. M. G., Ritsema, J., van Heijst, H. J., & Woodhouse, J. H. (2015). Joint inversion for global isotropic and radially anisotropic mantle structure including crustal thickness perturbations. *Journal of Geophysical Research: Solid Earth*, *120*, 4278–4300.

Chang, S. J., & Van der Lee, S. (2011). Mantle plumes and associated flow beneath Arabia and East Africa. *Earth and Planetary Science Letters*, *302*, 448–454.

Chesley, J. T., Rudnick, R. L., & Lee, C. T. (1999). Re-Os systematics of mantle xenoliths from the East African Rift: Age, structure, and history of the Tanzanian Craton. *Geochimica et Cosmochimica Acta*, *63*, 1203–1217.

Chorowicz, J. (2005). The east African rift system. *Journal of African Earth Sciences*, *43*, 379–410.

Civiero, C., Goes, S., Hammond, J. O. S., Fishwick, S., Ahmed, A., Ayele, A. . . . Stuart, G. W. (2016). Small-scale thermal upwellings under the northern East African Rift from S travel time tomography. *Journal of Geophysical Research: Solid Earth*, *121*, 7395–7408.

Corti, G., Iandelli, I., & Cerca, M. (2013). Experimental modeling of rifting at craton margins. *Geosphere*, *9*, 138–154.

Corti, G., van Wijk, J., Cloetingh, S., & Morley, C. K. (2007). Tectonic inheritance and continental rift architecture: Numerical and analogue models of the East African Rift system. *Tectonics*, *26*, TC6006.

Daly, M. C., Chorowicz, J., & Fairhead, J. D. (1989). Rift basin evolution in Africa: The influence of reactivated steep basement shear zones. *Geological Society*, *London*, *Special Publications*, *44*, 309–334.

Dawson, J. (1992). Neogene tectonics and volcanicity in the North Tanzania sector of the Gregory Rift Valley: Contrasts with the Kenya sector. *Tectonophysics*, *204*, 81–92.

De Waele, B., Liégeois, J. P., Nemchin, A. A., & Tembo, F. (2006). Isotopic and geochemical evidence of Proterozoic episodic crustal reworking within the Irumide Belt of south-central Africa, the southern metacratonic boundary of an Archaean Bangweulu Craton. *Precambrian Research*, *148*, 225–256.

Ebinger, C. J. (1989). Tectonic development of the western branch of the East African rift system. *Geological Society of America Bulletin*, *101*, 885–903.

Ebinger, C. (2005). Continental break-up: The East African perspective. *Astronomy & Geophysics*, *46*, 2–16.

Ebinger, C., Poudjom, Y., Mbede, E., Foster, F., & Dawson, J. (1997). Rifting Archean lithosphere: The Eyasi-Manyara-Natron rifts, East Africa. *Journal of the Geological Society London*, *154*, 947–960.

Fishwick, S., & Bastow, I. D. (2011). Towards a better understanding of African topography: A review of passive-source seismic studies of the African crust and upper mantle. *Geological Society*, *London*, *Special Publications*, *357*, 343–371.

Foster, A., Ebinger, C., Mbede, E., & Rex, D. (1997). Tectonic development of the northern Tanzanian sector of the East African Rift System. *Journal of the Geological Society London*, *154*, 689–700.

George, R., Rogers, N., & Kelley, S. (1998). Earliest magmatism in Ethiopia: Evidence for two mantle plumes in one flood basalt province. *Geology*, *26*, 923–926.

Gerya, T. V. (2010). *Introduction to numerical geodynamic modelling*. Cambridge, UK: Cambridge University Press, 358 pp.

Gerya, T. V., & Yuen, D. A. (2007). Robust characteristics method for modelling multiphase visco-elasto-plastic thermo-mechanical problems. *Physics of the Earth and Planetary Interiors*, *163*, 83–105.

Hansen, S. E., Nyblade, A. A., & Benoit, M. H. (2012). Mantle structure beneath Africa and Arabia from adaptively parameterized P-wave tomography: Implications for the origin of Cenozoic Afro-Arabian tectonism. *Earth and Planetary Science Letters*, *319*, 23–34.

Huismans, R. S., & Beaumont, C. (2007). Roles of lithospheric strain softening and heterogeneity in determining the geometry of rifts and continental margins. In G. D. Karner, G. D. Manatschal & L. M. Pinheiro (Eds.), *Imaging*, *mapping and modelling continental lithosphere extension and breakup*. *Geological Society*, *London*, *Special Publications*, *282*, 111–138.

Isola, I., Mazzarini, F., Bonini, M., & Corti, G. (2014). Spatial variability of volcanic features in early-stage rift settings: The case of the Tanzania Divergence, East African rift system. *Terra Nova*, *26*, 461–468.

Katumwehe, A. B., Abdelsalam, M. G., & Atekwana, E. A. (2015). The role of pre-existing Precambrian structures in rift evolution: The Albertine and Rhino grabens, Uganda. *Tectonophysics*, *646*, 117–129.

Keller, G. R., Khan, M. A., Morganc, P., Wendlandt, R. F., Baldridge, W. S., Olsen, K. H., . . . Braile, L. W. (1991). A comparative study of the Rio Grande and Kenya rifts. *Tectonophysics*, *197*, 355–371.

Keranen, K. M., Klemperer, S. L., Julia, J., Lawrence, J. F., & Nyblade, A. A. (2009). Low lower crustal velocity across Ethiopia: Is the main Ethiopian Rift a narrow rift in a hot craton? *Geochemistry Geophysics Geosystems*, *10*, Q0AB01.

Koptev, A., Burov, E., Calais, E., Leroy, S., Gerya, T., Guillou-Frottier, L., & Cloetingh, S. (2016). Contrasted continental rifting via plume-craton interaction: Applications to Central East African Rift. *Geoscience Frontiers*, *7*, 221–236.

Koptev, A., Burov, E., Gerya, T., Le Pourhiet, L., Leroy, S., Calais, E., & Jolivet, L. (2017). Plume-induced continental rifting and break-up in ultra-slow extension context: Insights from 3D numerical modeling. *Tectonophysics*, https://doi.org/10.1016/j.tecto.2017.03.025.

Koptev, A., Calais, E., Burov, E., Leroy, S., & Gerya, T. (2015). Dual continental rift systems generated by plume-lithosphere interaction. *Nature Geoscience*, *8*, 388–392.

Koptev, A., Cloetingh, S., Burov, E., François, T., & Gerya, T. (2017). Long-distance impact of Iceland plume on Norway's rifted margin. *Scientific Reports*, *7*, 10408.

Koptev, A. I., & Ershov, A. V. (2011). Thermal thickness of the Earth's lithosphere: A numerical model. *Moscow University Geology Bulletin*, *66*, 323–330.

Laó-Dávila, D. A., Al-Salmi, H. S., Abdelsalam, M. G., & Atekwana, E. A. (2015). Hierarchical segmentation of the Malawi Rift: The influence of inherited lithospheric heterogeneity and kinematics in the evolution of continental rifts. *Tectonics*, *34*, 2399–2417.

Le Gall, B., Gernigon, L., Rolet, J., Ebinger, C., Gloaguen, R., Nilsen, O., ... Mruma, A. (2004). Neogene-Holocene rift propagation in central Tanzania: Morphostructural and aeromagnetic evidence from the Kilombero area. *Geological Society of America Bulletin*, *116*, 490–510.

Le Gall, B., Nonnotte, P., Rolet, J., Benoit, M., Guillou, H., Mousseau-Nonnotte, M., ... Deverchère, J. (2008). Rift propagation at craton margin: Distribution of faulting and volcanism in the North Tanzanian Divergence (East Africa) during Neogene times. *Tectonophysics*, *448*, 1–19.

Lenoir, J. L., Liégeois, J. P., Theunissen, K., & Klerkx, J. (1994). The Palaeoproterozoic Ubendian shear belt in Tanzania: Geochronology and structure. *Journal of African Earth Sciences*, *19*, 169–184.

Manya, S. (2011). Nd-isotopic mapping of the Archaean–Proterozoic boundary in southwestern Tanzania: Implication for the size of the Archaean Tanzania Craton. *Gondwana Research*, *20*, 325–334.

McClusky, S., Reilinger, R., Mahmoud, S., Sari, D. B., & Tealeb, A. (2003). GPS constraints on Africa (Nubia) and Arabia plate motions. *Geophysical Journal International*, *155*, 126–138.

McConnell, R. B. (1972). Geological development of the rift system of eastern Africa. *Geological Society of America Bulletin*, *83*, 2549–2572.

Mechie, J., Keller, G. R., Prodehl, C., Khan, M. A., & Gaciri, S. J. (1997). A model for the structure, composition and evolution of the Kenya rift. *Tectonophysics*, *278*, 95–119.

Mohr, P. A. (1970). The Afar Triple Junction and sea-floor spreading. *Journal of Geophysical Research*, *75*, 7340–7352.

Mohr, P. (1982). Musings on continental rifts. In G. Palmason (Ed.), *Continental and oceanic rifts*. *American Geophysical Union Geodynamics Series*, *8*, 293–309.

Morley, C. K. (2010). Stress re-orientation along zones of weak fabrics in rifts: An explanation for pure extension in 'oblique' rift segments? *Earth and Planetary Science Letters*, *297*, 667–673.

Morley, C. K., Cunningam, S. M., Wescott, W. A., & Harper, R. M. (1999). Geology and geophysics of the Rukwa rift. In C. K. Morley (Ed.), *Geoscience of rift systems: Evolution of East Africa*. *AAPG Studies in Geology*, *44*, 91–110.

Morley, C. K., Wescott, W. A., Stone, D. M., Harper, R. M., Wigger, S. T., & Karanja, F. M. (1992). Tectonic evolution of the northern Kenyan Rift. *Journal of the Geological Society*, *149*, 333–348.

Mulibo, G. D., & Nyblade, A. A. (2013a). The P and S wave velocity structure of the mantle beneath eastern Africa and the African superplume anomaly. *Geochemistry, Geophysics, Geosystems*, *14*, 2696–2715.

Mulibo, G. D., & Nyblade, A. A. (2013b). Mantle transition zone thinning beneath eastern Africa: Evidence for a whole-mantle superplume structure. *Geophysical Research Letters*, *40*, 3562–3566.

Nolet, G., Karato, S. I., & Montelli, R. (2006). Plume fluxes from seismic tomography. *Earth and Planetary Science Letters*, *248*, 685–699.

Nyblade, A. A., Owens, T. J., Gurrola, H., Ritsema, J., & Langston, C. A. (2000). Seismic evidence for a deep upper mantle thermal anomaly beneath east Africa. *Geology*, *28*, 599–602.

Pasteels, P., Villeneuve, M., De Paepe, P., & Klerkx, J. (1989). Timing of the volcanism of the southern Kivu province: Implications for the evolution of the western branch of the East African Rift system. *Earth and Planetary Science Letters*, *94*, 353–363.

Pérez-Gussinyé, M., Metois, M., Fernández, M., Vergés, J., Fullea, J., & Lowry, A. R. (2009). Effective elastic thickness of Africa and its relationship to other proxies for lithospheric structure and surface tectonics. *Earth and Planetary Science Letters*, *287*, 152–167.

Pik, R., Marty, B., & Hilton, D. R. (2006). How many mantle plumes in Africa? The geochemical point of view. *Chemical Geology*, *226*, 100–114.

Ring, U. (1994). The influence of preexisting structure on the evolution of the Cenozoic Malawi Rift (East African Rift system). *Tectonics*, *13*, 313–326.

Ring, U. (2014). The East African rift system. *Austrian Journal Earth Sciences*, *107*, 132–146.

Ring, U., Betzler, C., & Delvaux, D. (1992). Normal vs. strike-slip faulting during rift development in East Africa: The Malawi rift. *Geology*, *20*, 1015–1018.

Ritsema, J., Nyblade, A. A., Owens, T. J., & Langston, C. A. (1998). Upper mantle seismic velocity structure beneath Tanzania, East Africa: Implications for the stability of cratonic lithosphere. *Journal of Geophysical Research*, *103*, 21201–21213.

Ritsema, J., van Heijst, H. J., & Woodhouse, J. H. (1999). Complex shear wave velocity structure imaged beneath Africa and Iceland. *Science*, *286*, 1925–1928.

Roberts, E. M., Stevens, N. J., O'Connor, P. M., Dirks, P. H. G. M., Gottfried, M. D., Clyde, W. C., ... Hemming, S. (2012). Initiation of the western branch of the East African Rift coeval with the eastern branch. *Nature Geoscience*, *5*, 289–294.

Rooney, T. O., Herzberg, C., & Bastow, I. D. (2012). Elevated mantle temperature beneath East Africa. *Geology*, *40*, 27–30.

Saria, E., Calais, E., Stamps, D. S., Delvaux, D., & Hartnady, C. J. H. (2014). Present-day kinematics of the East African Rift. *Journal of Geophysical Research*, *119*, 3584–3600.

Sippel, J., Meeßen, C., Cacace, M., Mechie, J., Fishwick, S., Heine, C. ... Strecker, M. R. (2017). The Kenya rift revisited: Insights into lithospheric strength through data-driven 3-D gravity and thermal modelling. *Solid Earth*, *8*, 45.

Smets, B., Delvaux, D., Ross, K. A., Poppe, S., Kervyn, M., d'Oreye, N., & Kervyn, F. (2016). The role of inherited crustal structures and magmatism in the development of rift segments: Insights from the Kivu basin, western branch of the East African Rift. *Tectonophysics*, *683*, 62–76.

Smith, M. (1994). Stratigraphic and structural constraints on mechanisms of active rifting in the Gregory Rift, Kenya. *Tectonophysics*, *236*, 3–22.

Stamps, D. S., Calais, E., Saria, E., Hartnady, C., Nocquet, J. M., Ebinger, C. J., & Fernandes, R. M. (2008). A kinematic model for the East African Rift. *Geophysical Research Letters*, *35*, LO5304

Theunissen, K., Klerkx, J., Melnikov, A., & Mruma, A. (1996). Mechanisms of inheritance of rift faulting in the western branch of the East African Rift, Tanzania. *Tectonics*, *15*, 776–790.

Versfelt, J., & Rosendahl, B. R. (1989). Relationships between pre-rift structure and rift architecture in Lakes Tanganyika and Malawi, East Africa. *Nature*, *337*, 354–357.

Weeraratne, D. S., Forsyth, D. W., Fischer, K. M., & Nyblade, A. A. (2003). Evidence for an upper mantle plume beneath the Tanzanian craton from Rayleigh wave tomography. *Journal of Geophysical Research: Solid Earth*, *108*, 2427.

Wenker, S., & Beaumont, C. (2016). Effects of lateral strength contrasts and inherited heterogeneities on necking and rifting of continents. *Tectonophysics*. https://doi.org/10.1016/j.tecto.2016.10.011

Williams, L. A. J. (1982). Physical aspects of magmatism in continental rifts. In: G. Pfilmason (Ed.), *Continental and oceanic rifts*. Geodynamic series (*Vol. 8*, pp. 193–222). Washington, DC: American Geophysical Union.

Zeyen, H., Volker, F., Wehrle, V., Fuchs, K., Sobolev, S. V., & Altherr, R. (1997). Styles of continental rifting: Crust-mantle detachment and mantle plumes. *Tectonophysics*, *278*, 329–352.

How to cite this article: Koptev A, Cloetingh S, Gerya T, Calais E, Leroy S. Non-uniform splitting of a single mantle plume by double cratonic roots: Insight into the origin of the central and southern East African Rift System. *Terra Nova*. 2018;30:125–134. https://doi.org/10.1111/ter.12317